Physica D 409 (2020) 132481

Contents lists available at ScienceDirect

Physica D

journal homepage: www.elsevier.com/locate/physd

Stable solitons in a nearly $\mathcal{PT}$-symmetric ferromagnet with spin-transfer torque

I.V. Barashenkov [a,b,*], Alexander Chernyavsky [a,c]

[a] Centre for Theoretical and Mathematical Physics, University of Cape Town, Rondebosch 7701, South Africa
[b] Joint Institute for Nuclear Research, Dubna, 141980, Russia
[c] Department of Mathematics and Statistics, University of Victoria, Victoria, BC V8P 5C2, Canada

ARTICLE INFO

Article history:
Received 23 November 2019
Received in revised form 6 March 2020
Accepted 20 March 2020
Available online 28 March 2020
Communicated by D. Pelinovsky

Keywords:
Spin torque oscillator
Landau–Lifshitz equation
Parity-time symmetry
Nonlinear Schroedinger equation
Solitons
Stability

ABSTRACT

We consider the Landau–Lifshitz equation for the spin torque oscillator — a uniaxial ferromagnet in an external magnetic field with polarised spin current driven through it. In the absence of the Gilbert damping, the equation turns out to be $\mathcal{PT}$-symmetric. We interpret the $\mathcal{PT}$-symmetry as a balance between gain and loss — and identify the gaining and losing modes. In the vicinity of the bifurcation point of a uniform static state of magnetisation, the $\mathcal{PT}$-symmetric Landau–Lifshitz equation with a small dissipative perturbation reduces to a nonlinear Schrödinger equation with a quadratic nonlinearity. The analysis of the Schrödinger dynamics demonstrates that the spin torque oscillator supports stable magnetic solitons. The $\mathcal{PT}$ near-symmetry is crucial for the soliton stability: the addition of a finite dissipative term to the Landau–Lifshitz equation destabilises all solitons that we have found.

1. Introduction

Conceived in the context of nonhermitian quantum mechanics [1], the idea of parity-time ($\mathcal{PT}$) symmetry has proved to be useful in the whole range of applied disciplines [2]. A $\mathcal{PT}$-symmetric structure is an open system where dissipative losses are exactly compensated by symmetrically arranged energy gain. In optics and photonics, systems with balanced gain and loss are expected to promote an efficient control of light, including all-optical low-threshold switching [3,4] and unidirectional invisibility [3,5,6]. There is a growing interest in the context of electronic circuitry [7], plasmonics [8], optomechanical systems [9], acoustics [10] and metamaterials [11].

This study is concerned with yet another area where the gain-loss balance gives rise to new structures and behaviours, namely, the magnetism and spintronics. In contrast to optics and nanophotonics, where the nonhermitian effects constitute a well-established field of study, the research into $\mathcal{PT}$-symmetric magnetic systems is still in its early stages, with only a handful of models set up over the last several years.

One of the systems proposed in the literature comprises two coupled ferromagnetic films, one with gain and the other one with loss [12]. (For an experimental implementation of this structure, see [13].) A related concept consists of a pair of parallel magnetic nanowires, with counter-propagating spin-polarised currents [14]. In either case the corresponding mathematical model is formed by two coupled Landau–Lifshitz equations, with $\mathcal{PT}$ symmetry being realised as a symmetry between the corresponding magnetisation vectors. A two-spin Landau–Lifshitz system gauge-equivalent to the $\mathcal{PT}$-symmetric nonlocal Schrödinger equation is also a member of this class of models [15].

An independent line of research concerned the dynamics of a single spin under the action of the spin-transfer torque. Projecting the magnetisation vector onto the complex plane stereographically and modelling the spin torque by an imaginary magnetic field [16], Galda and Vinokur have demonstrated the $\mathcal{PT}$-symmetry of the resulting nonhermitian Hamiltonian [17]. (For the generalisation to spin chains, see [18]; the nonreciprocal spin transfer is discussed in [19].) Unlike the two-component structures of Refs [12–14], the $\mathcal{PT}$-symmetry of the spin torque oscillator of Galda and Vinokur is an intrinsic property of an individual spin. It results from the system's invariance under the simultaneous time reversal and the imaginary magnetic field flip [17].

The structure we consider in this paper shares a number of similarities with the spin torque oscillator of Refs [17,18]. (There is also a fair number of differences.) It consists of two ferromagnetic layers separated by a conducting film (Fig. 1).

* Corresponding author at: Centre for Theoretical and Mathematical Physics, University of Cape Town, Rondebosch 7701, South Africa.
E-mail addresses: Igor.Barashenkov@uct.ac.za (I.V. Barashenkov), chernya@uvic.ca (A. Chernyavsky).

https://doi.org/10.1016/j.physd.2020.132481
0167-2789/

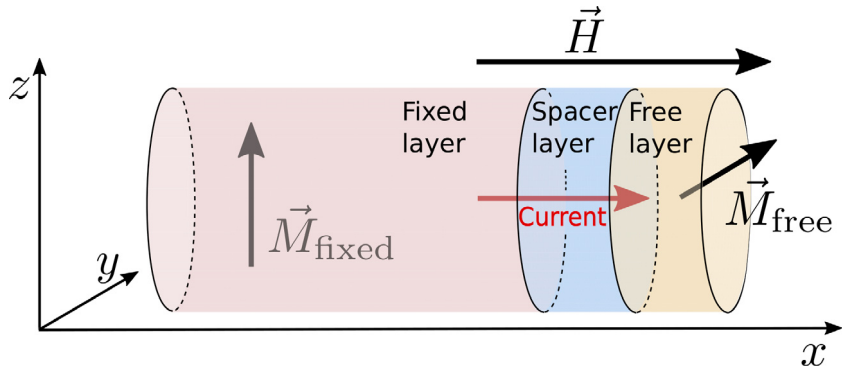

Fig. 1. A schematic of the spin torque oscillator. An electric current flows through a nanowire with two ferromagnetic layers. In the thick layer (on the left) the magnetisation is fixed (through large volume, large anisotropy or pinning by additional underlayers). This causes a polarisation of the passing electron spins. The polarised current exerts torque on the thin layer (on the right) where the magnetisation is governed by the Landau–Lifshitz equation (1).

The spin-polarised current flows from a layer with fixed magnetisation to a layer where the magnetisation vector is free to rotate [16,20].

A one-dimensional uniaxial classical ferromagnet in the external magnetic field is described by the Landau–Lifshitz equation [16,20] (also known as the Landau–Lifshitz–Gilbert–Słonczewski equation in the current context):

$$\dot{\mathbf{M}} = -\mathbf{M}\times\mathbf{M}'' - \mathbf{M}\times\mathbf{H} - \beta(\mathbf{M}\cdot\hat{\mathbf{z}})\mathbf{M}\times\hat{\mathbf{z}} - \gamma\mathbf{M}\times\mathbf{M}\times\hat{\mathbf{z}} + \lambda\mathbf{M}\times\dot{\mathbf{M}}. \tag{1}$$

Here the overdot stands for the time derivative and the prime indicates the derivative with respect to x. In equation (1), the variables have been non-dimensionalised so that the magnetisation vector $\mathbf{M} = (M_x, M_y, M_z)$ lies on a unit sphere: $\mathbf{M}^2 = 1$. The magnetic field is taken to be constant and directed horizontally: $\mathbf{H} = (H_0, 0, 0)$. The anisotropy axis is z, with $\hat{\mathbf{z}} = (0, 0, 1)$. The positive and negative constant β corresponds to the easy-axis and easy-plane anisotropy, respectively. (Note that the authors of [17,18] considered the ferromagnet anisotropic along the x axis.) The fourth term on the right-hand side of (1) – the Słonczewski term – accounts for the spin transfer by the current that passes through an external ferromagnetic layer that has a fixed magnetisation in the direction $\hat{\mathbf{z}}$. The last term is the Gilbert damping term. The damping coefficient λ is positive; the field H_0 and the current amplitude γ can also be chosen positive without loss of generality.

In this paper, we study the nonlinear dynamics of localised solutions of equation (1), both with small and finite-strength damping.

A class of soliton solutions of equation (1) was obtained by Hoefer, Silva and Keller [21]. The solitons discovered by those authors are dissipative analogs of the Ivanov–Kosevich *magnon droplets* [22]. (For the experimental realisation, see [23].) Our setup has a different geometry from the one of Hoefer et al. One difference is that we consider the magnetic layer with a parallel anisotropy while the magnon droplets require a perpendicular one [21–23]. An additional distinction is that our vector $\mathbf{H}$ is orthogonal to the direction of the fixed magnetisation — while the magnetic field in Ref [21] was not. Because of the different geometry, the Landau–Lifshitz equation of Ref [21] does not exhibit the $\mathcal{PT}$ invariance. The dissipative magnon droplets are sustained through the competition of torque and damping, the two actors represented by terms of different mathematical forms — rather than by a symmetric balance of two similar but oppositely-directed effects.

Another class of localised structures in the spin torque oscillator is commonly referred to as the *standing spin wave bullets*. These have been theoretically predicted by Slavin and Tiberkevich [24] — outside the context of the Landau–Lifshitz equation. (For the experimental realisation, see [25].) The spin wave bullets are found in the magnetic layer with parallel anisotropy, when the magnetic field is directed parallel to the fixed layer's magnetisation. The direction of the vector $\mathbf{H}$ is what makes our geometry different from the setup considered in Ref [24]. Like the magnon droplets, the spin wave bullets are sustained by an asymmetric balance of the spin torque and finite-strength damping.

The paper is organised as follows. We start with the demonstration of the gain-loss balance in the Landau–Lifshitz equation with the vanishing Gilbert damping. This $\mathcal{PT}$-symmetric system and systems that are close to it will prove to have special properties in this paper, where we consider equations both with small and finite λ. In Section 3 we classify stability and bifurcation of four nonequivalent stationary states with uniform magnetisation. Three of those states are found to be admissible as stable backgrounds for localised structures. In the vicinity of the bifurcation points, the dynamics of the localised structures are governed by quadratic Schrödinger or Ginsburg–Landau equations, depending on whether the Gilbert damping is weak or finite-strength (Section 4). Despite the absence of the dissipative terms, our quadratic Schrödinger equations are not conservative; however one of them obeys the $\mathcal{PT}$-symmetry. Both Ginsburg–Landau equations and their Schrödinger counterparts – $\mathcal{PT}$-symmetric or not – support two types of soliton solutions. We show that either of these types is only stable in the $\mathcal{PT}$-symmetric situation (Sections 5–6). Section 7 summarises results of this study.

2. Gain-loss balance in the absence of Gilbert losses

Equation (1) is nonconservative due to the presence of the spin torque and Gilbert's dissipative term. In spin torque oscillators, solitons are expected to exist due to the energy supplied by torque being offset by finite-strength dissipation [21]. However when $\lambda = 0$, the spin hamiltonian modelling our structure is $\mathcal{PT}$-symmetric [17] and therefore some form of the gain-loss balance should occur in this case as well, despite the absence of the Gilbert damping. To uncover the gain-loss competition intrinsic to the spin torque, we define two complex fields, $u(x, t)$ and $v(x, t)$, related to the magnetisation vector $\mathbf{M}$ via the Hopf map:

$$M_x = v^*u + u^*v, \quad M_y = i(u^*v - v^*u), \quad M_z = |u|^2 - |v|^2. \tag{2}$$

When the magnetisation is spatially uniform, $\partial\mathbf{M}/\partial x = 0$, the equation (1) with $\lambda = 0$ can be reformulated as a nonlinear

Schrödinger dimer:

$$iu_t + \frac{H_0}{2}v + \frac{\beta}{2}(|u|^2 - |v|^2)u = i\gamma|v|^2u, \tag{3}$$

$$iv_t + \frac{H_0}{2}u - \frac{\beta}{2}(|u|^2 - |v|^2)v = -i\gamma|u|^2v. \tag{4}$$

According to equations (3)–(4), the external energy is fed into the u-mode and dissipated by its v counterpart. The magnetic field H_0 couples u to v, carrying out the energy exchange between the two modes.

The sustainability of the gain-loss balance in the system (3)–(4) is reflected by its invariance under the product of the $\mathcal{P}$ and $\mathcal{T}$ transformations. Here the inversion $\mathcal{P}$ swaps the two modes around,

$$\mathcal{P}: \quad u \to v, \quad v \to u, \tag{5}$$

while $\mathcal{T}$ represents the reflection of time:

$$\mathcal{T}: \quad t \to -t, \quad u \to u^*, \quad v \to v^*. \tag{6}$$

These transformations admit a simple formulation in terms of the components of magnetisation (2):

$$\mathcal{P}: \quad M_y \to -M_y, \quad M_z \to -M_z \tag{7}$$

and

$$\mathcal{T}: \quad t \to -t, \quad M_y \to -M_y. \tag{8}$$

The involutions (7) and (8) remain relevant in the analysis of equation (1) with the x-dependent magnetisation. Here one can either leave the parity operation in the form (7) or include the inversion of the x coordinate in this transformation:

$$\mathcal{P}: \quad x \to -x, \quad M_y \to -M_y, \quad M_z \to -M_z. \tag{9}$$

Writing the vector equation (1) in the component form,

$$\begin{cases} \dot{M}_x = & M_zM_y'' - M_yM_z'' - \beta M_yM_z \\ & -\gamma M_xM_z + \lambda(M_y\dot{M}_z - M_z\dot{M}_y), \\ \dot{M}_y = & M_xM_z'' - M_zM_x'' - H_0M_z + \beta M_xM_z \\ & -\gamma M_yM_z + \lambda(M_z\dot{M}_x - M_x\dot{M}_z), \\ \dot{M}_z = & M_yM_x'' - M_xM_y'' + H_0M_y \\ & +\gamma(M_x^2 + M_y^2) + \lambda(M_x\dot{M}_y - M_y\dot{M}_x), \end{cases} \tag{10}$$

one readily checks that in the conservative limit ($\gamma = \lambda = 0$), the Landau–Lifshitz equation is invariant under the $\mathcal{P}$- and $\mathcal{T}$-involutions individually. The equation with the spin torque term added ($\gamma \neq 0$) is invariant under the product ($\mathcal{PT}$) transformation only. Accordingly, the equation with the γ-term is a $\mathcal{PT}$-symmetric extension of the conservative Landau–Lifshitz equation. Finally, the addition of the Gilbert damping term ($\lambda \neq 0$) breaks the $\mathcal{PT}$-symmetry.

3. Uniform static states

The uniform static states are space- and time-independent solutions of equation (1) satisfying $\mathbf{M}^2 = 1$. These are given by fixed points of the dynamical system

$$\begin{cases} \dot{M}_x = -\beta M_yM_z - \gamma M_xM_z + \lambda(M_y\dot{M}_z - M_z\dot{M}_y), \\ \dot{M}_y = (\beta M_x - H_0 - \gamma M_y)M_z + \lambda(M_z\dot{M}_x - M_x\dot{M}_z), \\ \dot{M}_z = H_0M_y + \gamma(M_x^2 + M_y^2) + \lambda(M_x\dot{M}_y - M_y\dot{M}_x) \end{cases} \tag{11}$$

on the surface of the unit sphere.

Once a fixed point $\mathbf{M}^{(0)}$ has been determined, we let $\mathbf{M} = \mathbf{M}^{(0)} + \delta\mathbf{M}$, linearise the system (10) in $\delta\mathbf{M}$, and consider solutions of the form

$$\delta\mathbf{M} = \mathbf{m}\, e^{\mu t - ikx}, \tag{12}$$

where $\mathbf{m} = (m_x, m_y, m_z)^T$ is a real constant vector and k a real wavenumber that may take values from $-\infty$ to ∞. We call the uniform static state unstable if at least one of the roots μ of the associated characteristic equation has a positive real part in some interval of k. Otherwise the state is deemed stable.

Since equation (1) conserves the quantity $\mathbf{M}^2$, the difference between $\left(\mathbf{M}^{(0)}\right)^2$ and the square of the vector $\mathbf{M}^{(0)} + \delta\mathbf{M}$ will be time-independent:

$$\frac{\partial}{\partial t}\left(2\,\delta\mathbf{M}\cdot\mathbf{M}^{(0)}\right) = 0.$$

Substituting from (12) and assuming $\mu \neq 0$, this gives

$$\mathbf{m}\cdot\mathbf{M}^{(0)} = 0. \tag{13}$$

Equation (13) implies (a) that the time-dependent perturbations of the uniform static states lie on the unit sphere; and (b) that the characteristic equation may not have more than two nonzero roots, μ_1 and μ_2. The third root (μ_3) has to be zero.

Apart from classifying stability of the uniform static states, it is useful to know which of these solutions can serve as backgrounds to static magnetic solitons. To weed out a priori unsuitable cases, we set $\mu = 0$ in the characteristic equation and consider k^2 as a new unknown (rather than a parameter that varies from 0 to ∞). If all roots $(k^2)_n$ of the resulting equation are real positive, there can be no localised solutions asymptotic to the uniform static state $\mathbf{M}^{(0)}$ as $x \to \pm\infty$. On the other hand, if there is at least one negative or complex root, the solution $\mathbf{M}^{(0)}$ remains a candidate for solitons' background.

3.1. Equatorial fixed points on the unit sphere

One family of time-independent solutions of the system (11) describes a circle on the (M_x, M_y)-plane:

$$M_x^2 + \left(M_y + \frac{H_0}{2\gamma}\right)^2 = \frac{H_0^2}{4\gamma^2}, \quad M_z = 0.$$

Imposing the constraint $\mathbf{M}^2 = 1$ leaves us with just two members of the family:

$$M_x^{(0)} = \pm\sqrt{1 - \gamma^2/H_0^2}, \quad M_y^{(0)} = -\gamma/H_0, \quad M_z^{(0)} = 0. \tag{14}$$

In the system with $\gamma \neq 0$, these fixed points are born as H_0 is increased through the value $H_0 = \gamma$. Since the points (14) lie on the equator of the unit sphere, we will be referring to them simply as the *equatorial* fixed points, the eastern ($M_x^{(0)} > 0$) and the western ($M_x^{(0)} < 0$) one. Fig. 2(a) depicts the equatorial fixed points in the phase portrait of the dynamical system (11).

Linearising equation (1) about the uniform static state corresponding to an equatorial fixed point, we obtain two nonzero stability eigenvalues

$$\mu_{1,2} = \frac{-\lambda(2K - \beta) \pm \sqrt{\lambda^2\beta^2 - 4K(K - \beta)}}{2(1 + \lambda^2)}, \tag{15a}$$

$$K = k^2 + H_0M_x^{(0)}. \tag{15b}$$

Making use of (15) it is not difficult to see that in the easy-plane or isotropic ferromagnet (i.e. in the situation where $\beta \leq 0$), the eastern uniform static state ($M_x^{(0)} > 0$) is stable irrespective of the choice of γ, λ and H_0. On the other hand, when the anisotropy is easy-axis ($\beta > 0$), the eastern state is stable if

$$H_0 \geq \sqrt{\beta^2 + \gamma^2} \tag{16}$$

and unstable otherwise.

To check the suitability of the eastern uniform static state as a background for solitons, we set $\mu = 0$ in the expression (15a); this transforms it into a quadratic equation for k^2. When

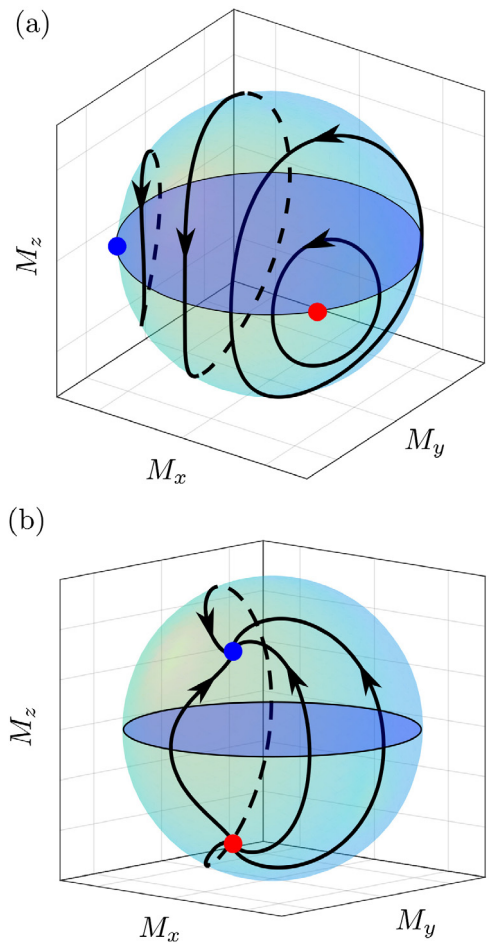

Fig. 2. The phase portrait of the dynamical system (11) with $H_0 > \sqrt{\beta^2+\gamma^2}$ (a) and $H_0 < \gamma$ (b). In (a), two dots on the equator of the unit sphere mark the fixed points of the vector field: the western (blue) and eastern point (red). In (b), the blue dot indicates the northern and the red dot the southern fixed point. Apart from the fixed points, the figures show a few representative trajectories; physically, these correspond to spatially-uniform evolutions of magnetisation. (The portraits in (a) and (b) are for $\lambda = 0$.). (For interpretation of the references to colour in this figure legend, the reader is referred to the web version of this article.)

$\beta < \sqrt{H_0^2-\gamma^2}$, both roots of this equation are negative: $k^2 = -\sqrt{H_0^2-\gamma^2}$ and $k^2 = \beta - \sqrt{H_0^2-\gamma^2}$. This implies that there is a pair of exponentials $\exp(-ik_{1,2}x)$ decaying to zero as $x \to -\infty$ and another pair decaying as $x \to +\infty$. Therefore the uniform static state (14) with $M_x^{(0)} > 0$ can serve as a background to solitons for any set of parameters $\beta, \gamma, H_0, \lambda$ in its stability domain.

Turning to the west-point solution ($M_x^{(0)} < 0$ in equation (14)), a simple analysis of the eigenvalues (15) indicates that there are wavenumbers k such that $\mathrm{Re}\,\mu > 0$ for any quadruplets of β, γ, H_0 and λ. Hence the western uniform static state is always unstable. We are not considering it any further.

3.2. Latitudinal fixed points

Another one-parameter family of constant solutions of equation (1) forms a vertical straight line in the M_x, M_y, M_z-space:

$$M_x = \frac{H_0\beta}{\beta^2+\gamma^2}, \quad M_y = -\frac{H_0\gamma}{\beta^2+\gamma^2}, \quad -\infty < M_z < \infty.$$

The substitution of the above coordinates into $\mathbf{M}^2 = 1$ selects two fixed points on the unit sphere:

$$M_x^{(0)} = \frac{H_0\beta}{\beta^2+\gamma^2}, \quad M_y^{(0)} = -\frac{H_0\gamma}{\beta^2+\gamma^2},$$
$$M_z^{(0)} = \pm\sqrt{1-\frac{H_0^2}{\beta^2+\gamma^2}}. \tag{17}$$

Since these points lie above and below the equatorial (M_x, M_y)-plane, we will be calling them the *latitudinal* fixed points: the northern ($M_z^{(0)} > 0$) and the southern ($M_z^{(0)} < 0$) point. See Fig. 2(b).

In the anisotropic equation ($\beta \neq 0$) the northern and southern points are born as H_0 is decreased through $\sqrt{\beta^2+\gamma^2}$. In this case, there is a parameter interval $\gamma < H_0 < \sqrt{\beta^2+\gamma^2}$ where two pairs of fixed points, latitudinal and equatorial, coexist.

The bifurcation diagram for the isotropic equation is different. When $\beta = 0$, the latitudinal fixed points (17) emerge as the eastern and western points (14) converge and split out of the equatorial plane. In this case, there is just one pair of uniform static states for any $H_0 \neq \gamma$: the equatorial pair for $H_0 > \gamma$ and the latitudinal pair for $H_0 < \gamma$.

The linearisation of equation (1) about the uniform static state corresponding to the latitudinal fixed-point (17) gives

$$\mu_{1,2} = -\frac{\lambda Q + \gamma M_z^{(0)} \pm \sqrt{\frac{1}{4}\lambda^2\beta^2h^2 - P(P-\beta h)}}{1+\lambda^2}, \tag{18}$$

where

$$P = k^2 + \beta - \gamma\lambda M_z^{(0)}, \quad Q = k^2 + \beta\left(1-\frac{h}{2}\right)$$

and

$$h = \frac{H_0^2}{\beta^2+\gamma^2}. \tag{19}$$

A simple analysis demonstrates that when $\beta \geq 0$, the north-point solution ($M_z^{(0)} > 0$ in (17)) is stable regardless of the values of $\lambda \geq 0$, H_0 and $\gamma > 0$. As for the easy-plane anisotropy ($\beta < 0$), the northern uniform static state is stable only when the inequalities $\lambda \leq \lambda_c$ and $H_0 \leq H_c$ are satisfied simultaneously. Here

$$\lambda_c = \frac{\gamma}{|\beta|}\frac{\sqrt{1-h}}{1-h/2} \tag{20}$$

and

$$H_c = \sqrt{\frac{2\gamma(\beta^2+\gamma^2)}{\beta^2}\left(\sqrt{\beta^2+\gamma^2}-\gamma\right)}. \tag{21}$$

Note that H_c is smaller than $\sqrt{\gamma^2+\beta^2}$; hence the region $H_0 \leq H_c$ lies entirely within the northern point's existence domain (defined by the inequality $H_0 < \sqrt{\gamma^2+\beta^2}$).

Finally, we consider the eigenvalues pertaining to the southern uniform static state ($M_z^{(0)} < 0$ in (17)). Our conclusion here is that in the isotropic and easy-plane ferromagnet ($\beta \leq 0$), this solution is unstable regardless of the choice of other parameters. In the easy-axis situation ($\beta > 0$), the southern state is stable if $\lambda \geq \lambda_c$ with λ_c as in (20) — and unstable otherwise.

To determine the parameter region where the north- and south-point solutions can serve as backgrounds for solitons, we set $\mu = 0$ in equation (18). In each of the two cases, the resulting quadratic equation for k^2 has two positive roots only if $\beta < 0$ is satisfied along with the inequality $H_0 > H_c$, where H_c is as in (21). This is the only no-go region for solitons. Outside this region, the quadratic equation has either two negative or two

Table 1
Stability of four fixed-point solutions of equation (1).

	$\beta < 0$	$\beta = 0$	$\beta > 0$
Eastern	Stable	Stable	Stable if $H_0 \geq \sqrt{\beta^2 + \gamma^2}$
Western	Unstable	Unstable	Unstable
Northern	Stable if $\lambda \leq \lambda_c$ and $H_0 \leq H_c$	Stable	Stable
Southern	Unstable	Unstable	Stable if $\lambda \geq \lambda_c$

complex roots; the corresponding uniform static states can serve as solitons' asymptotes.

The bottom line is that either of the two latitudinal uniform static states is suitable as a background for solitons in its entire stability domain.

3.3. Summary of uniform static states

For convenience of the reader, the stability properties of the constant solutions corresponding to the four fixed points are summed up in Table 1.

Before turning to the perturbations of these uniform static states, it is worth noting their symmetry properties. Each of the equatorial states is $\mathcal{PT}$-symmetric in the sense that each of these two solutions is invariant under the product of the transformations (9) and (8). In contrast, neither of the two latitudinal states is invariant; the $\mathcal{PT}$ operator maps the northern solution to southern and the other way around. The different symmetry properties of the equatorial and longitudinal solutions will give rise to different invariances of equations for their small perturbations.

4. Slow dynamics near bifurcation points

4.1. Perturbation of equatorial fixed point

Consider the eastern point in the pair of equatorial fixed points (14):

$$\mathbf{M}^{(0)} = \left(\sqrt{1 - \frac{\gamma^2}{H_0^2}}, -\frac{\gamma}{H_0}, 0\right). \tag{22}$$

We assume that the parameters β, γ, λ and H_0 lie in the stability domain of the uniform static state (22).

The plane orthogonal to the vector $\mathbf{M}^{(0)}$ is spanned by the vectors

$$\mathbf{A} = (0, 0, 1), \quad \mathbf{B} = \left(\frac{\gamma}{H_0}, \sqrt{1 - \frac{\gamma^2}{H_0^2}}, 0\right).$$

The unit vector $\mathbf{M}$ can be expanded over the orthonormal triplet $\{\mathbf{A}, \mathbf{B}, \mathbf{M}^{(0)}\}$:

$$\mathbf{M} = \eta\mathbf{A} + \xi\mathbf{B} + \chi\mathbf{M}^{(0)}.$$

Letting $\mathbf{M}(x, t) \to \mathbf{M}^{(0)}$ as $x \to \pm\infty$, the coefficient fields η, ξ and χ have the following asymptotic behaviour:

$$\eta \to 0, \ \xi \to 0, \ \chi \to 1 \text{ as } |x| \to \infty.$$

The complex field $\Psi = \xi + i\eta$ satisfies

$$i\dot{\Psi} = \chi\Psi'' - \Psi\chi'' + \lambda(\Psi\dot{\chi} - \chi\dot{\Psi}) - \sqrt{H_0^2 - \gamma^2}\Psi + \gamma(\chi - i\eta\xi - 1 + \eta^2) + i\beta\eta\chi, \tag{23}$$

where $\chi = \sqrt{1 - |\Psi|^2}$ while the prime and overdot indicate the derivative with respect to x and t, respectively. Note that when $\lambda = 0$, equation (23) is $\mathcal{PT}$-symmetric, that is, invariant under a composite transformation consisting of three involutions: $t \to -t$, $x \to -x$, and $\Psi \to \Psi^*$.

Assume that H_0 is close to the bifurcation point of the uniform static state (22) – that is, H_0 is slightly greater than γ. In this case, Ψ will depend on a hierarchy of slow times $T_n = \epsilon^n t$ and stretched spatial coordinates $X_n = \epsilon^{n/2}x$, where $n = 1, 3, 5, \ldots$ and the small parameter ϵ is defined by

$$\epsilon^2 = 1 - \frac{\gamma^2}{H_0^2}.$$

In the limit $\epsilon \to 0$ the new coordinates become independent so we can write

$$\frac{\partial}{\partial t} = \epsilon D_1 + \epsilon^3 D_3 + \cdots;$$
$$\frac{\partial^2}{\partial x^2} = \epsilon\partial_1^2 + 2\epsilon^2\partial_1\partial_3 + \epsilon^3(\partial_3^2 + 2\partial_1\partial_5) + \cdots,$$

where $D_n = \partial/\partial T_n$ and $\partial_n = \partial/\partial X_n$. Assume, in addition, that the anisotropy constant β is of order ϵ and let $\beta = \epsilon\mathcal{B}$ with $\mathcal{B} = O(1)$. Considering small η and ξ, we expand

$$\Psi = \epsilon\psi_1 + \epsilon^3\psi_3 + \cdots.$$

Substituting the above expansions in (23), we equate coefficients of like powers of ϵ. The order ϵ^2 gives a Ginsburg–Landau type of equation with a quadratic nonlinearity:

$$(i + \lambda)D_1\psi - \partial_1^2\psi + \frac{\gamma}{2}\psi^2 = -\gamma\psi + \frac{\mathcal{B}}{2}(\psi - \psi^*). \tag{24}$$

(Here ψ is just a short-hand notation for ψ_1.)

Note that in the derivation of (24) we took λ to be $O(1)$. If we, instead, let $\lambda = O(\epsilon)$, the dissipative term would fall out of equation (24) and we would end up with a nonlinear Schrödinger equation:

$$iD_1\psi - \partial_1^2\psi + \frac{\gamma}{2}\psi^2 = -\gamma\psi + \frac{\mathcal{B}}{2}(\psi - \psi^*). \tag{25}$$

The quadratic Schrödinger equation (25) does not have the U(1) phase invariance. However, the equation is $\mathcal{PT}$-symmetric, that is, invariant under the composite map $t \to -t$, $x \to -x$, $\psi \to \psi^*$. As we will see in Section 5, this discrete symmetry is enough to stabilise solitons.

4.2. Perturbation of latitudinal fixed points

Choosing the background in the form of one of the two latitudinal fixed points

$$\mathbf{M}^{(0)} = \left(\frac{\beta}{H_0}h, -\frac{\gamma}{H_0}h, \pm\sqrt{1 - h}\right), \tag{26}$$

we let $\mathbf{M}(x, t)$ approach the same point $\mathbf{M}^{(0)}$ as $x \to \pm\infty$. In (26), h is defined by equation (19).

As in the previous subsection, we expand the magnetisation vector over an orthonormal basis $\{\mathbf{A}, \mathbf{B}, \mathbf{M}^{(0)}\}$:

$$\mathbf{M} = \eta\mathbf{A} + \xi\mathbf{B} + \chi\mathbf{M}^{(0)}, \tag{27}$$

where, this time,

$$\mathbf{A} = \left(\mp\frac{\beta}{H_0}\sqrt{h(1-h)}, \pm\frac{\gamma}{H_0}\sqrt{h(1-h)}, \sqrt{h}\right)$$

and

$$\mathbf{B} = \left(\frac{\gamma}{H_0}\sqrt{h}, \frac{\beta}{H_0}\sqrt{h}, 0\right).$$

We assume that H_0 is close to the bifurcation point where the northern and southern fixed points are born (that is, H_0 is slightly smaller than $\sqrt{\beta^2+\gamma^2}$) and define a small parameter ϵ:

$$h = 1 - \epsilon^2.$$

As in the analysis of the equatorial fixed points, we let $\beta = \epsilon\mathcal{B}$, where $\mathcal{B} = O(1)$. Assuming that the magnetisation $\mathbf{M}$ is just a small perturbation of $\mathbf{M}^{(0)}$, we expand the small coefficients in (27) in powers of ϵ:

$$\eta = \epsilon\eta_1 + \epsilon^3\eta_3 + \cdots, \quad \xi = \epsilon\xi_1 + \epsilon^3\xi_3 + \cdots .$$

The constraint $\eta^2 + \xi^2 + \chi^2 = 1$ implies then

$$\chi = 1 - \epsilon^2\frac{\eta_1^2+\xi_1^2}{2} + \cdots .$$

Substituting these expansions in the Landau–Lifshitz equation (10) and equating coefficients of like powers of ϵ, the order ϵ^2 gives

$$D_1\xi_1 = \partial_1^2\eta_1 - \lambda D_1\eta_1 - \gamma(\eta_1\xi_1 \pm \xi_1)$$

and

$$D_1\eta_1 = \lambda D_1\xi_1 - \partial_1^2\xi_1 + \mathcal{B}\xi_1 \mp \gamma\eta_1 - \frac{\gamma}{2}(\eta_1^2 - \xi_1^2).$$

The above two equations can be combined into a single equation for the complex function $\psi = \xi_1 + i\eta_1$:

$$(i+\lambda)D_1\psi - \partial_1^2\psi + \frac{\gamma}{2}\psi^2 = \mp i\gamma\psi - \frac{\mathcal{B}}{2}(\psi + \psi^*). \tag{28}$$

The Ginsburg–Landau equation (28) resembles equation (24) governing the dynamics near the equatorial uniform static state; however there is an important difference. Namely, even if we let $\lambda = 0$ in (28) [that is, even if we assume that the damping is $O(\epsilon)$ or weaker in the Landau–Lifshitz–Gilbert equation (1)], the resulting nonlinear Schrödinger equation will *not* become $\mathcal{PT}$-symmetric. This fact will have important repercussions for the stability of solitons.

5. Soliton excitations of equatorial state

Letting

$$u(x,t) = -\frac{1}{3}\psi(X_1,T_1), \quad x = \frac{\sqrt{\gamma}}{2}X_1, \quad t = \frac{\gamma}{4}T_1, \tag{29}$$

the Ginsburg–Landau equation (24) is cast in the form

$$(i+\lambda)u_t - u_{xx} - 6u^2 = -4u + b(u - u^*), \tag{30}$$

where $b = 2\mathcal{B}/\gamma$. (We alert the reader that the scaled variables x and t do not coincide with the original x and t of the Landau–Lifshitz equation (1). We are just re-employing the old symbols in a new context here.)

In the present section we consider localised solutions of equation (30) approaching 0 as $|x| \to \infty$. Regardless of λ, the zero solution is stable if $b \le 2$ and unstable otherwise. This inequality agrees with the stability range (16) of the eastern uniform static state within the original Landau–Lifshitz equation. (Note that the term $-bu^*$ plays the role of the parametric driver in (30) [26]; the above stability criterion states that the zero solution cannot sustain drivers with amplitudes b greater than 2.)

5.1. Fundamental soliton and its stability

Eq. (30) has a stationary soliton solution:

$$u_s = \mathrm{sech}^2 x. \tag{31}$$

To distinguish it from localised modes with internal structure, we refer to this solution as the *fundamental soliton* — or simply *sech mode*. Letting

$$u(x,t) = u_s(x) + \varepsilon[f(x) + ig(x)]e^{\mu t}$$

and linearising in small ε, we obtain an eigenvalue problem

$$\mu(g - \lambda f) = \mathcal{H}f, \tag{32a}$$

$$-\mu(f - \lambda g) = (\mathcal{H} - 2b)g, \tag{32b}$$

with the operator

$$\mathcal{H} = -d^2/dx^2 + 4 - 12\,\mathrm{sech}^2 x. \tag{33}$$

The vector eigenvalue problem (32) is reducible to a scalar eigenvalue problem of the form

$$(\mathcal{H} - b + \mu\lambda)^2 g + (\mu^2 - b^2)g = 0.$$

The stability exponents μ are roots of the quadratic equation

$$(E - b + \mu\lambda)^2 + \mu^2 - b^2 = 0,$$

where E is an eigenvalue of the operator $\mathcal{H}$: $\mathcal{H}y = Ey$. The two roots are

$$\mu^{(\pm)} = \frac{\lambda(b-E) \pm \sqrt{\lambda^2 b^2 + E(2b-E)}}{1+\lambda^2}. \tag{34}$$

The eigenvalues of the Pöschl–Teller operator (33) are $E_0 = -5$, $E_1 = 0$, and $E_2 = 3$, with the eigenfunctions $y_0 = \mathrm{sech}^3 x$, $y_1 = \mathrm{sech}^2 x \tanh x$ and $y_2 = \mathrm{sech}\, x\left(1 - \frac{5}{4}\mathrm{sech}^2 x\right)$, respectively. The continuous spectrum occupies the semiaxis $E_{\mathrm{cont}} \ge 4$, with the edge eigenfunction given by $y_3 = \tanh x\left(1 - \frac{5}{3}\tanh^2 x\right)$. For each eigenvalue E_n, $n = 0, 1, 2$, equation (34) yields two roots, $\mu_n^{(+)}$ and $\mu_n^{(-)}$.

In the analysis of the roots (34) we need to distinguish between two situations: damped ($\lambda > 0$) and undamped one ($\lambda = 0$). Assume, first, that $\lambda > 0$ and let, in addition, $b \ge 0$. It is not difficult to check that the root $\mu_n^{(+)}$ will have a positive real part provided the corresponding eigenvalue E_n satisfies $E_n < 2b$. On the other hand, the set of three eigenvalues of the operator (33) does include a negative eigenvalue (E_0) that satisfies $E_0 < 2b$ regardless of the particular value of $b \ge 0$. Therefore the soliton has an exponent $\mu_0^{(+)}$ with $\mathrm{Re}\,\mu_0^{(+)} > 0$ for any $b \ge 0$.

In the case where $\lambda > 0$ but $b < 0$, the root $\mu_n^{(+)}$ will have a positive real part provided E_n satisfies $E_n < 0$. As in the previous case, this inequality is satisfied by the eigenvalue E_0 so that the soliton has an exponent with $\mathrm{Re}\,\mu_0^{(+)} > 0$ for any $b < 0$.

We conclude that the fundamental soliton of equation (30) is unstable in the presence of damping — regardless of the sign and magnitude of the anisotropy coefficient b. Fig. 3 illustrates the evolution of a weakly perturbed soliton in the Ginsburg–Landau equation with $\lambda \ne 0$.

Turning to the situation with $\lambda = 0$ we assume, first, that $b > 0$. The equations (34) will give a pair of opposite real roots $\mu_n^{(\pm)}$ if the corresponding eigenvalue satisfies $0 < E_n < 2b$ — and a pair of pure imaginary roots otherwise. The only positive eigenvalue of the operator (33) is $E_2 = 3$; it satisfies the above inequality if $b > 3/2$. The range of b where the roots are imaginary is, therefore, $0 < b \le 3/2$.

In the situation where $\lambda = 0$ but $b < 0$, the pair of opposite exponents $\mu_n^{(\pm)}$ is real if E_n falls in the interval $2b < E_n < 0$ and pure imaginary if E_n lies outside this interval. The only negative eigenvalue is $E_0 = -5$; it falls in the interval in question if $b < -5/2$. The complementary range $-5/2 \le b < 0$ corresponds to the imaginary roots.

Finally, in the isotropic ferromagnet ($b = 0$) the stability exponents are all pure imaginary: $\mu_n^{(\pm)} = \pm iE_n$.

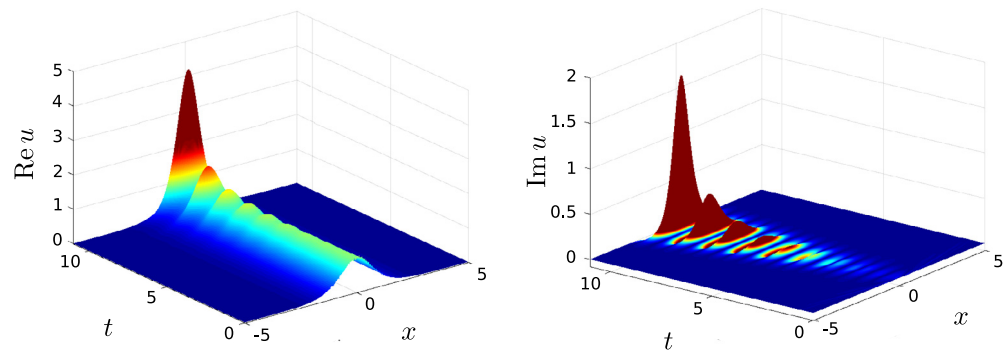

Fig. 3. Instability of the fundamental soliton in the presence of damping. This evolution was obtained by the direct numerical simulation of equation (30) with $b = 0$ and $\lambda = 0.1$. The initial condition was in the form of the soliton (31) perturbed by a random perturbation within 5% of the soliton's amplitude. The spatial interval of simulation was $(-58, 58)$; in the plot it has been cut down for visual clarity.

Merging the three ranges where all exponents are pure imaginary produces the stability domain of the undamped fundamental soliton in terms of the anisotropy-to-current ratio:

$$-\frac{5}{2} \le b \le \frac{3}{2}. \tag{35}$$

5.2. Twisted modes in isotropic ferromagnet

The Ginsburg–Landau equation (30) with $b = 0$ admits an additional pair of localised solutions:

$$u_{\mathrm{T}} = 2\mathrm{sech}^2(2x) \pm 2i\,\mathrm{sech}(2x)\tanh(2x). \tag{36}$$

The modulus of $u_{\mathrm{T}}(x)$ is bell-shaped while its phase grows or decreases by π as x changes from $-\infty$ to $+\infty$. The solution looks like a pulse twisted by 180° in the $(\mathrm{Re}\,u, \mathrm{Im}\,u)$-plane. In what follows, we refer to each of the solutions (36) as a *twisted*, or simply *sech-tanh*, mode.

Linearising equation (30) about the twisted mode (36) and assuming that the small perturbation depends on time as $e^{\mu t}$, we arrive at an eigenvalue problem

$$\mathcal{L}f(X) = -\frac{\mu}{4}(\lambda + i)f(X) \tag{37}$$

for the Schrödinger operator with the Scarff-II complex potential:

$$\mathcal{L} = -\frac{d^2}{dX^2} + 1 - 6\mathrm{sech}^2 X \mp 6i\,\mathrm{sech}\,X\tanh X. \tag{38}$$

In (37)–(38), $X = 2x$.

The $\mathcal{PT}$-symmetric operator (38) has an all-real spectrum including three discrete eigenvalues [27]. Let y_n be the eigenfunction associated with an eigenvalue E_n: $\mathcal{L}y_n = E_n y_n$. The eigenvalue–eigenfunction pairs are then given by

$$E_0 = -\frac{5}{4}, \quad y_0 = (\mathrm{sech}^2 X \pm i\,\mathrm{sech}X\tanh X)^{3/2};$$
$$E_1 = 0, \quad y_1 = \mathrm{sech}X(\mathrm{sech}X \pm i\tanh X)^2, \tag{39}$$

and $E_2 = 3/4$ with

$$y_2 = (3 \pm 2i\sinh X)(\mathrm{sech}^2 X \pm i\,\mathrm{sech}X\tanh X)^{3/2}. \tag{40}$$

Each of the eigenvalues E_n gives rise to a stability exponent

$$\mu_n = 4\frac{i - \lambda}{1 + \lambda^2}E_n$$

in equation (37). When the dissipation coefficient $\lambda > 0$, the exponent pertaining to the negative eigenvalue E_0 has a positive real part. Accordingly, the twisted modes (36) are unstable in the presence of damping. In contrast, when $\lambda = 0$, all exponents μ_n $(n = 0, 1, 2)$ are pure imaginary so the twisted modes are stable.

5.3. Oscillatory modes

An interesting question is whether there are any other stable localised structures — in particular, in the situation where Eq. (30) has zero damping. Fig. 4 illustrates the evolution of a gaussian initial condition $u(x, 0) = \exp(-x^2)$ that can be seen as a nonlinear perturbation of the soliton (31). The gaussian evolves into an oscillatory localised structure (a kind of a breather) which remains close to the soliton (31) — but does not approach it as $t \to \infty$. This observation suggests that Eq. (30) with $\lambda = 0$ has a family of stable time-periodic spatially localised solutions, with the stationary soliton (31) being just a particular member of the family.

It is fitting to note that the existence of breather families is common to nonlinear $\mathcal{PT}$-symmetric equations [28]. Breathers prevail among the products of decay of generic localised initial conditions [28,29].

5.4. Stable solitons in two dimensions

We close this section with a remark on the Landau–Lifshitz–Gilbert–Słonczewski equation in two dimensions:

$$\frac{\partial \mathbf{M}}{\partial t} = -\mathbf{M} \times \nabla^2\mathbf{M} - \mathbf{M} \times \mathbf{H} - \beta(\mathbf{M}\cdot\hat{\mathbf{z}})\mathbf{M} \times \hat{\mathbf{z}}$$
$$- \gamma\mathbf{M} \times \mathbf{M} \times \hat{\mathbf{z}} + \lambda\mathbf{M} \times \frac{\partial \mathbf{M}}{\partial t}. \tag{41}$$

Here $\nabla^2 = \frac{\partial^2}{\partial x^2} + \frac{\partial^2}{\partial y^2}$. Assuming that H_0 is only slightly above γ and that the anisotropy β and damping λ are small, we consider a perturbation of the east-point uniform state (22). Following the asymptotic procedure outlined in Section 4.1, equation (41) is reducible in this limit to a planar Schrödinger equation:

$$iu_t = u_{xx} + u_{yy} + 6u^2 - 4u + b(u - u^*), \tag{42}$$

where

$$b = \frac{2H_0}{\gamma}\frac{\beta}{\sqrt{H_0^2 - \gamma^2}}.$$

Like its one-dimensional counterpart (25), equation (42) is $\mathcal{PT}$-symmetric. The $\mathcal{PT}$-operation can be chosen, for instance, in the form

$$t \to -t, \quad x \to -x, \quad y \to -y, \quad u \to u^*.$$

The quadratic Schrödinger equation (42) has a static radially-symmetric soliton solution,

$$u_s(x, y) = \mathcal{R}(r), \tag{43}$$

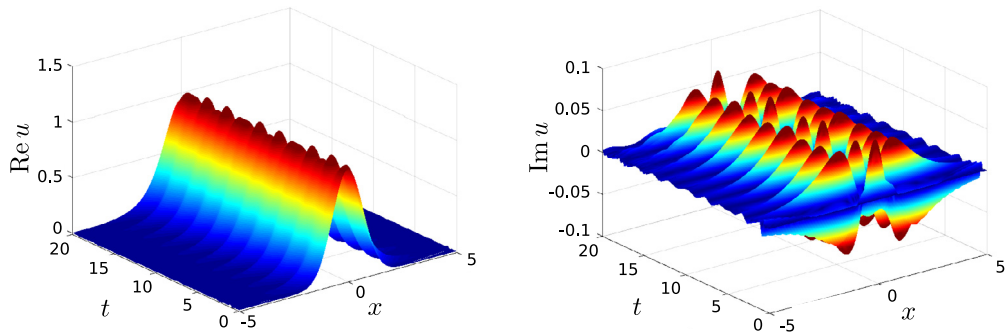

Fig. 4. The evolution of the initial condition in the form of a gaussian, $u(x,0) = \exp(-x^2)$, in equation (30) with $\lambda = 0$ and $b = 0$. Left panel: $\mathrm{Re}\, u$; right panel: $\mathrm{Im}\, u$. The emerging solution is a breather with a small imaginary part and the real part close to the soliton (31). Note that the figure shows only a portion of the full simulation interval $(-58, 58)$.

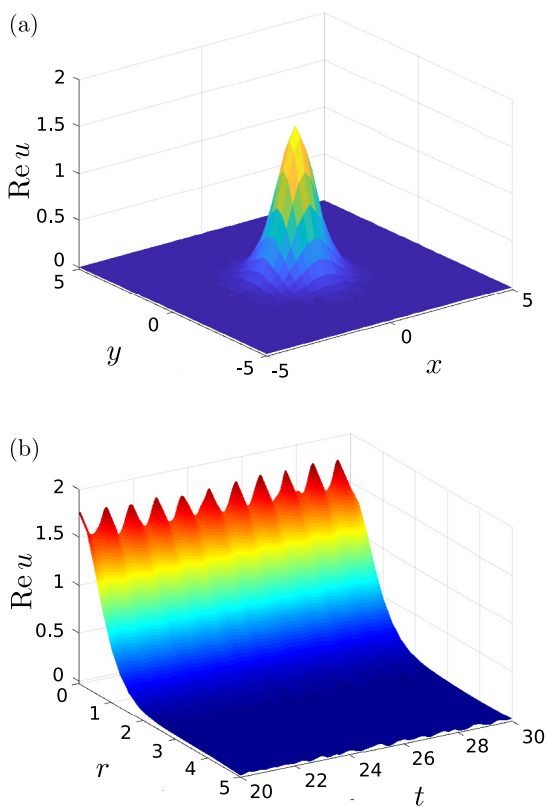

Fig. 5. Localised solutions of the quadratic Schrödinger equation on the plane: the stationary soliton (a) and a breather (b). Both figures were produced by direct numerical simulations of equation (42) with $b = 0$. In panel (a), the initial condition was taken in the form of the soliton (43) perturbed by a random perturbation within 5% of its amplitude. After $t = 100$, the solution (shown in the panel) remains close to the soliton. In panel (b), the initial condition was chosen as $u = 1.6\exp(-r^2)$. After an initial transient, the solution settles to a localised oscillatory state shown in the figure.

where $\mathcal{R}(r)$ is a nodeless (bell-shaped) solution of the boundary-value problem

$$\mathcal{R}_{rr} + \frac{1}{r}\mathcal{R}_r - 4\mathcal{R} + 6\mathcal{R}^2 = 0,$$
$$\mathcal{R}_r(0) = 0, \quad \mathcal{R}(r) \to 0 \text{ as } r \to \infty.$$

Postponing the detailed stability analysis of the soliton (43) to future publications, we restrict ourselves to the simplest case of isotropic ferromagnet, $b = 0$. A numerical simulation of equation (42) with the initial condition in the form of the noise-perturbed soliton (43) indicates that the soliton is stable against small perturbations. [See Fig. 5(a).] On the other hand, generic localised initial conditions evolve into time-periodic breather-like states [Fig. 5(b)]. This suggests that the quadratic Schrödinger equation (42) — and hence the planar Landau–Lifshitz equation (41) — support a broad class of stable stationary and oscillatory localised structures.

6. Soliton excitations of latitudinal state

The scaling transformation (29) takes the equations (28) to the nondimensional form:

$$(i+\lambda)u_t - u_{xx} - 6u^2 = \mp 4iu - b(u+u^*). \tag{44}$$

As in Section 5, $b = 2\mathcal{B}/\gamma$ here.

In what follows, we confine ourselves to the analysis of the isotropic equations ($b = 0$) as it is the only regime where we were able to obtain soliton solutions of equations (44). In the isotropic case, the $u = 0$ solution of the top-sign equation in (44) is stable while the same solution of the bottom-sign equation is unstable — regardless of whether λ is zero or not. (This agrees with the stability properties of the north and south fixed-point solutions of the Landau–Lifshitz equation; see Section 3.2.) Hence we only keep the top-sign equation in what follows.

6.1. Sech mode

Letting $b = 0$, the top-sign equation in (44) can be further transformed to

$$(1-i\lambda)w_t = w_{zz} - 4w + 6w^2, \tag{45}$$

where

$$w(z,t) = -iu(x,t), \quad z = e^{i\pi/4}x. \tag{46}$$

An obvious static solution of equation (45) is $w_s = \mathrm{sech}^2 z$; the corresponding solution of the original equation (44) is

$$u_s(x) = i\,\mathrm{sech}^2\left(e^{i\frac{\pi}{4}}x\right). \tag{47}$$

The solution (47) decays to zero as $x \to \pm\infty$ and does not have singularities on the real line. Similar to the solution (31) over the equatorial background, we term the solution (47) the *sech soliton*.

To classify the stability of the soliton (47), we linearise equation (45) about $w_s = \mathrm{sech}^2 z$. Assuming that the small perturbation depends on time as $e^{\mu t}$, we obtain

$$\mu = -\frac{1+i\lambda}{1+\lambda^2}E, \tag{48}$$

where E is an eigenvalue of the Pöschl–Teller operator

$$\mathcal{H} = -\frac{d^2}{dz^2} + 4 - 12\,\mathrm{sech}^2 z.$$

The operator acts upon functions $y(z)$ defined on the line $z = e^{i\pi/4}\xi$ $(-\infty < \xi < \infty)$ on the complex-z plane and satisfying the boundary conditions $y \to 0$ as $\xi \to \pm\infty$.

As discussed in the previous section, the equation $\mathcal{H}y = Ey$ with $E = -5$ has a solution $y_0 = \text{sech}^3 z$. The function $\text{sech}^3(e^{i\pi/4}\xi)$ is nonsingular for all $-\infty < \xi < \infty$ and decays to zero as $\xi \to \pm\infty$; hence $E_0 = -5$ is a discrete eigenvalue of the operator $\mathcal{H}$. The corresponding exponent μ in (48) has a positive real part regardless of λ. This implies that the *sech* soliton (47) is unstable irrespective of whether λ is zero or not.

6.2. sech-tanh modes

Applying the transformation (46) to a pair of solutions

$$w_{\rm T} = 2\text{sech}^2(2z) \pm 2i\,\text{sech}(2z)\tanh(2z) \tag{49}$$

of equation (45), we obtain two localised solutions of the original equation (44):

$$u_{\rm T} = \mp 2\,\text{sech}(2e^{i\pi/4}x)\tanh(2e^{i\pi/4}x) + 2i\,\text{sech}^2(2e^{i\pi/4}x). \tag{50}$$

By analogy with solutions (36) over the equatorial background, we are referring to (50) as the *sech-tanh modes*.

Linearising equation (45) about each of its stationary solutions (49) and assuming that the small perturbation depends on time as $e^{\mu t}$, we obtain the following equation for the exponent μ:

$$\mu = -4\frac{1+i\lambda}{1+\lambda^2}E.$$

Here E is an eigenvalue of the Scarff-II operator:

$$\mathcal{L}y = Ey, \tag{51a}$$

$$\mathcal{L} = -\frac{d^2}{dZ^2} + 1 - 6\,\text{sech}^2 Z \mp 6i\,\text{sech}Z\tanh Z, \tag{51b}$$

with $Z = 2z$. The eigenvalue problem (51) is posed on the line

$$Z = e^{i\pi/4}\xi, \quad -\infty < \xi < \infty \tag{52}$$

on the complex-Z plane, with the boundary conditions $y \to 0$ as $\xi \to \pm\infty$.

Three solutions of equation (51a) are in (39)–(40). Since $y_n(Z)$ $(n = 0, 1, 2)$ are nonsingular and decay to zero as Z tends to infinity in either direction along the line (52), these solutions are eigenfunctions of the operator $\mathcal{L}$ — and the corresponding E_n are the eigenvalues. The exponent μ_0 pertaining to the eigenvalue $E_0 = -5/4$ has a positive real part:

$$\mu_0 = -4\frac{1+i\lambda}{1+\lambda^2}E_0.$$

Consequently, the *sech-tanh* modes (50) are unstable — no matter whether λ is zero or not.

6.3. Summary of one-dimensional solitons

The stability properties of six localised modes supported by the quadratic Ginsburg–Landau equations (30) and (44) are summarised in Table 2. The Table includes two *sech* solitons (the fundamental soliton (31) and its latitudinal-background counterpart, equation (47)) and four *sech-tanh* modes (the twisted modes (36) and their latitudinal analogs (50)).

Table 2
Stability of the stationary nonlinear modes in one dimension. The middle column classifies solutions of equation (30) while the right-hand column corresponds to solutions of (44).

	Over equatorial background	Over latitudinal background (with $b = 0$)
sech soliton	Stable if $\lambda = 0$ and $-\frac{5}{2} < b < \frac{3}{2}$	Unstable
sech-tanh modes	Exist if $b = 0$; Stable if $\lambda = 0$	Unstable

7. Concluding remarks

We have studied nonlinear structures associated with the spin torque oscillator — an open system described by the Landau–Lifshitz–Gilbert–Słonczewski equation. In the limit of zero damping ($\lambda = 0$), this nonconservative system is found to be $\mathcal{PT}$-symmetric. The *nearly-$\mathcal{PT}$* symmetric equation corresponds to small nonzero λ. In this paper, we have considered both nearly-symmetric and nonsymmetric oscillators (small and moderate λ).

The spin torque oscillator has four stationary states of uniform magnetisation; they are described by four fixed points on the unit **M**-sphere. Two of these states have their magnetisation vectors lying in the equatorial plane of the unit sphere while the other two correspond to fixed points in the northern and southern hemisphere, respectively. We have assumed that the external magnetic field H_0 has been tuned to values ϵ^2-close to the bifurcation points of the "equatorial" and "latitudinal" uniform static states, and that the ferromagnet is only weakly anisotropic: $\beta = O(\epsilon)$. In that limit, small-amplitude localised perturbations of the uniform static states satisfy the Ginsburg–Landau equations — equations (30) and (44), respectively.

If the damping coefficient λ is $O(\epsilon)$ or smaller, each of the two Ginsburg–Landau reductions becomes a quadratic nonlinear Schrödinger equation. Of the two Schrödinger equations, the one corresponding to perturbations of the "equatorial" uniform static state turns out to be $\mathcal{PT}$-symmetric. (Thus the asymptotic reduction of a *nearly* $\mathcal{PT}$-symmetric Landau–Lifshitz system is *exactly* $\mathcal{PT}$-symmetric.) This Schrödinger equation proves to be quite remarkable. Indeed, despite both our Ginsburg–Landau reductions supporting soliton solutions, it is only in the $\mathcal{PT}$-symmetric Schrödinger limit that the solitons are found to be stable.

The $\mathcal{PT}$-symmetric Schrödinger equation supports two types of stable solitons. The constant-phase solution (31) is stable in an ϵ-wide band of β values, extending from the easy-axis to easy-plane region. [The stability band is demarcated by the inequality (35).] On the other hand, a pair of stable solitons with the twisted phase, equations (36), is only supported by the nearly-isotropic ferromagnet: $\beta = O(\epsilon^2)$ or smaller. In addition to stable static solitons, the $\mathcal{PT}$-symmetric Schrödinger equation exhibits stable breathers.

In the two-dimensional geometry, the Landau–Lifshitz equation for the spin torque oscillator admits an asymptotic reduction to a planar quadratic Schrödinger equation, equation (42). Like its one-dimensional counterpart, the $\mathcal{PT}$-symmetric planar Schrödinger equation has stable static and oscillatory soliton solutions.

Finally, it is worth re-emphasising here that the $\mathcal{PT}$-symmetric Schrödinger equation is a reduction of the whole family of nearly-$\mathcal{PT}$ symmetric Landau–Lifshitz–Gilbert–Słonczewski equations with $\lambda = O(\epsilon)$ — and not just of its special case with $\lambda = 0$. Therefore our conclusion on the existence of stable solitons is applicable to the physically relevant class of spin torque oscillators with nonzero damping.

CRediT authorship contribution statement

I.V. Barashenkov: Conceptualization, Methodology, Formal analysis, Writing - original draft, Writing - review & editing, Funding acquisition. **Alexander Chernyavsky:** Conceptualization, Formal analysis, Software, Visualization, Writing - review & editing.

Acknowledgements

We thank Boris Ivanov and Andrei Slavin for useful discussions. This project was supported by the NRF of South Africa (Grant Nos. 105835, 120844 and 120467).

References

[1] C.M. Bender, S. Boettcher, Phys. Rev. Lett. 80 (1998) 5243;
C.M. Bender, S. Boettcher, P.N. Meisinger, J. Math. Phys. 40 (1999) 2201;
C.M. Bender, Contemp. Phys. 46 (2005) 277;
C.M. Bender, Rep. Prog. Phys. 70 (2007) 947.
[2] D. Christodoulides, R. El-Ganainy, U. Peschel, S. Rotter (Eds.), Focus on parity-time symmetry in optics and photonics, New J. Phys. (2015-2017);
V. Kovanis, J. Dionne, D. Christodoulides, A. Desyatnikov (Eds.), Issue on parity time photonics, IEEE J. Sel. Top. Quantum Electron. 22 (5) (2016).
[3] H. Ramezani, T. Kottos, R. El-Ganainy, D.N. Christodoulides, Phys. Rev. A 82 (2010) 043803.
[4] M. Kulishov, J.M. Laniel, N. Blanger, J. Azaa, D.V. Plant, Opt. Express 13 (2005) 3068;
A.A. Sukhorukov, Z.Y. Xu, S. Yu Kivshar, Phys. Rev. A 82 (2010) 043818;
Z. Lin, H. Ramezani, T. Eichelkraut, T. Kottos, H. Cao, D. Christodoulides, Phys. Rev. Lett. 106 (2011) 213901.
[5] A. Regensburger, C. Bersch, M.-A. Miri, G. Onishchukov, D.N. Christodoulides, U. Peschel, Nature 488 (2012) 167.
[6] L. Feng, Y.-L. Xu, W.S. Fegadolli, M.-H. Lu, J.E.B. Oliveira, V.R. Almeida, Y.-F. Chen, A. Scherer, Nature Mater. 12 (2012) 108;
L.L. Sánchez-Soto, J.J. Monzon, Symmetry 6 (2014) 396.
[7] J. Schindler, Z. Lin, J.M. Lee, H. Ramezani, F.M. Ellis, T. Kottos, J. Phys. A 45 (2012) 444029;
H. Ramezani, J. Schindler, F.M. Ellis, U. Gunther, T. Kottos, Phys. Rev. A 85 (2012) 062122;
Z. Lin, J. Schindler, F.M. Ellis, T. Kottos, Phys. Rev. A 85 (2012) 050101;
N. Bender, S. Factor, J.D. Bodyfelt, H. Ramezani, D.N. Christodoulides, F.M. Ellis, T. Kottos, Phys. Rev. Lett. 110 (2013) 234101.
[8] H. Benisty, A. Degiron, A. Lupu, A. De Lustrac, S. Chénais, S. Forget, M. Besbes, G. Barbillon, A. Bruyant, S. Blaize, G. Lérondel, Opt. Express 19 (2011) 18004;
M. Mattheakis, Th. Oikonomou, M.I. Molina, G.P. Tsironis, IEEE J. Sel. Top. Quantum Electron. 22 (2015) 5000206.
[9] H. Jing, Ş. K. Özdemir, Z. Geng, J. Zhang, X.-Y. Lü, B. Peng, L. Yang, F. Nori, Sci. Rep. 5 (2015) 9663;
K.V. Kepesidis, T.J. Milburn, J. Huber, K.G. Makris, S. Rotter, P. Rabl, New J. Phys. 18 (2016) 095003.
[10] X. Zhu, H. Ramezani, C. Shi, J. Zhu, X. Zhang, Phys. Rev. X 4 (2014) 031042;
R. Fleury, D. Sounas, A. Alu, Nat. Commun. 6 (2015) 5905.
[11] N. Lazarides, G.P. Tsironis, Phys. Rev. Lett. 110 (2013) 053901.
[12] J.M. Lee, T. Kottos, B. Shapiro, Phys. Rev. B 91 (2015) 094416.
[13] H. Liu, D. Sun, C. Zhang, M. Groesbeck, R. Mclaughlin, Z. Valy Vardeny, Sci. Adv. 5 (2019) eaax9144.
[14] V.V. Konotop, J. Yang, D.A. Zezyulin, Rev. Modern Phys. 88 (2016) 035002.
[15] T.A. Gadzhimuradov, A.M. Agalarov, Phys. Rev. A 93 (2016) 062124.
[16] M. Lakshmanan, Phil. Trans. R. Soc. A 369 (2011) 1280.
[17] A. Galda, V.M. Vinokur, Phys. Rev. B 94 (2016) 020408(R).
[18] A. Galda, V.M. Vinokur, Phys. Rev. B 97 (2018) 201411(R).
[19] A. Galda, V.M. Vinokur, Sci. Rep. 9 (2019) 17484.
[20] M.D. Stiles, J. Miltat, Spin dynamics in confined magnetic structures III, in: Topics in Applied Physics, vol. 101, Springer, Berlin, 2006, pp. 225–308;
D.C. Ralph, M.D. Stiles, J. Magn. Magn. Mater. 320 (2008) 1190–1216;
A. Slavin, V. Tiberkevich, IEEE Trans. Magn. 45 (2009) 1875-1918;
I.D. Mayergoyz, G. Bertotti, C. Serpico, Nonlinear Magnetisation Dynamics in Nanosystems, Elsevier, 2009;
J.-V. Kim, Solid State Physics 63, Elsevier, 2012, pp. 217–294;
Z. Zeng, G. Finocchio, H. Jiang, Nanoscale 5 (2013) 2219-2231;
J. Åkerman, Spin transfer torque driven magnetodynamical solitons, in: Topology in Magnetism, in: Springer Series in Solid-State Sciences, vol. 192, Springer, Cham, 2018, pp. 335–356.
[21] M.A. Hoefer, T.J. Silva, M.W. Keller, Phys. Rev. B 82 (2010) 054432.
[22] B.A. Ivanov, A.M. Kosevich, JETP Lett 24 (1976) 454;
B.A. Ivanov, A.M. Kosevich, Zh. Eksp. Teor. Fiz. 72 (1977) 2000;
A.M. Kosevich, B.A. Ivanov, A.S. Kovalev, The magnon droplets are reviewed, Phys. Rep. 194 (1990) 117;
A.M. Kosevich, B.A. Ivanov, A.S. Kovalev, Nonlinear waves of magnetisation, in: Dynamical and Topological Solitons, Naukova Dumka, Kiev, 1983.
[23] S.M. Mohseni, et al., Science 339 (2013) 1295;
D. Backes, F. Maciá, S. Bonetti, R. Kukreja, H. Ohldag, A.D. Kent, Phys. Rev. Lett. 115 (2015) 127205.
[24] A. Slavin, V. Tiberkevich, Phys. Rev. Lett. 95 (2005) 237201.
[25] S. Bonetti, V. Tiberkevich, G. Consolo, G. Finocchio, P. Muduli, F. Mancoff, A. Slavin, J. Åkerman, Phys. Rev. Lett. 105 (2010) 217204.
[26] I.V. Barashenkov, M.M. Bogdan, V.I. Korobov, Europhys. Lett. 15 (1991) 113;
S. Longhi, Opt. Lett. 20 (1995) 695.
[27] Z. Ahmed, Phys. Lett. A 282 (2001) 343;
Z. Ahmed, Phys. Lett. A 287 (2001) 295.
[28] I.V. Barashenkov, S.V. Suchkov, A.A. Sukhorukov, S.V. Dmitriev, Y.S. Kivshar, Phys. Rev. A 86 (2012) 053809.
[29] N.V. Alexeeva, I.V. Barashenkov, A.A. Sukhorukov, Y.S. Kivshar, Phys. Rev. A 85 (2012) 063837;
N.V. Alexeeva, I.V. Barashenkov, Y.S. Kivshar, New J. Phys. 19 (2017) 113032.